Dynamics of a Sodium Chloride Ion Pair in Water

Omar A. Karim and J. Andrew McCammon*

Contribution from the Department of Chemistry, University of Houston—University Park, Houston, Texas 77004. *Received September 24, 1985*

Abstract: A sodium chloride ion pair in water has quasi-stable states in which the ions are in contact or are separated by one or more bridging water molecules. The dynamics of the transitions between these two states have been explored by computer simulation. The transitions have a sluggish, diffusional character because the ion motions are concerted with the rearrangement of many water molecules in their hydration shells. Two types of separation mechanism are prominent. In one of these, a water molecule from the first hydration shell of chloride interacts with water in the first shell around sodium and is drawn into a bridging position between the ions. In the other mechanism, a water molecule in the first shell around sodium interacts directly with the chloride ion and is subsequently drawn into a bridging position.

The association or dissociation of ion pairs in solution is an important step in many chemical reactions and in noncovalent interactions such as the formation of chemical or biochemical complexes.[1-8] For a detailed understanding of such processes, one needs answers to many fundamental questions. For example, what is the free energy of an ion pair–solvent system as a function of the ion–ion distance? What are the rate constants for ion pair association and dissociation? What role does the solvent structure and dynamics play in determining the behavior of ion pairs? A number of theoretical and simulation studies have focused on such questions.[9-27]

Quite recently, we have begun to explore some of these questions by means of computer simulation of the atomic motions in a simple model system comprising two ions, sodium and chloride, dissolved in water. In the initial work, the free energy of this system was computed for a range of ion–ion separations.[28] The free energy was found to have two local minima, corresponding to contact and solvent-separated ion pairs, respectively. A low barrier lies between these minima. Subsequently, the equilibrium solvation structure of this system has been studied in detail.[29] In the present work, we begin a study of the dynamics of this system, with special emphasis on the nature of the transitions between the contact and solvent-separated ion pairs.

This paper is organized as follows: We first describe the computer model that is used and briefly review the equilibrium calculations. Subsequently, the method for investigating the dynamics is detailed. The results are then presented and analyzed and possible directions of future work are suggested.

Table I. Specifications of Model[a]

TIPS2 site	q	$10^{-3}A^2$, kcal Å^{12}/mol	C^2, kcal Å^6/mol
O in H_2O	0.000	695	600
M in H_2O	−1.070	0	0
H in H_2O	0.535	0	0
Na^+	1.0	14	300
Cl^-	−1.0	26 000	3500

[a] System: number of H_2O = 295, number of ions = 2, box length = 25.46 Å, and box width = 18.62 Å. Radial interaction cutoff for equilibrium calculations = 7.5 Å. Radial interaction cutoff for dynamics calculations = 7.89 Å. Strength of confining umbrella potential used in dynamics = 0.24 × 10^3 kcal Å^{-2} mol^{-1}.

Methods

Computer Model. The system chosen for study consists of a sodium chloride ion pair in a box of 295 water molecules. The box is rectangular, and periodic boundary conditions are applied to the water molecules only. The ions are kept well away from the boundaries of the box in order to minimize "image" effects. The specifications of the system are given in Table I.

We have used the TIPS2 model for water throughout our calculations. This model, as well as the ion parameters used here, are due to Jorgensen, et al.[30,31] The TIPS2 is a rigid four-center model for water. The algorithm SHAKE[32] is used to enforce the constraints. There are three charges in this water molecule, two on the hydrogens and one located on the HOH bisector but not at the location of the oxygen atom. The actual potentials that operate are shown in the following functional form:

$$V_{WW}^{LJ} = \sum_{i<j} [A_W^2/r_{ij}^{12} - C_W^2/r_{ij}^6] \quad (1)$$

$$V_{WW}^{Coul} = \sum_{i<j} \sum_{\text{sites}} q_i q_j / r_{ij} \quad (2)$$

(1) Masnovi, J. M.; Levine, A.; Kochi, J. K. *J. Am. Chem. Soc.* **1985**, *107*, 4356.
(2) Friedman, H. L. *Annu. Rev. Phys. Chem.* **1981**, *32*, 179; *Pure Appl. Chem.* **1981**, *53*, 1277.
(3) Enderby, J. E.; Neilson, G. W. *Rep. Prog. Phys.* **1981**, *44*, 593.
(4) Warshel, A. *Acc. Chem. Res.* **1981**, *14*, 284.
(5) Manning, G. S. *Acc. Chem. Res.* **1981**, *14*, 284.
(6) Kessler, H.; Feigel, M. *Acc. Chem. Res.* **1982**, *15*, 2.
(7) Simon, J. D.; Peters, K. S. *J. Am. Chem. Soc.* **1982**, *104*, 6542.
(8) Neumann, E. "Structural and Functional Aspects of Enzyme Catalysis"; Eggerer H., Huber, R., Eds.; Springer Verlag: Berlin, 1981.
(9) Kusalik, P. G.; Patey, G. N. *J. Chem. Phys.* **1983**, *79*, 4468 and references therein.
(10) Pettitt, B. M.; Rossky, P. J.; McCammon, J. A., to be published.
(11) Friedman, H. L. *Methods in Enzymology*, in press.
(12) Wolynes, P. G. *J. Chem. Phys.* **1978**, *68*, 473.
(13) Colonomos, P.; Wolynes, P. G. *J. Chem. Phys.* **1979**, *71*.
(14) Hubbard, J. B.; Colonomos, P.; Wolynes, P. G. *J. Chem. Phys.* **1979**, *71*.
(15) Marchese, F. T.; Beveridge, D. L. *J. Am. Chem. Soc.* **1984**, *106*, 3713.
(16) Geiger, A. *Ber. Bunsen-Ges. Phys. Chem.* **1981**, *85*, 52-63.
(17) Ciccotti, G.; Turq, P.; Lantelme, F. *Chem. Phys.* **1984**, *88*, 333-338.
(18) Calef, D. F.; Wolynes, P. G. *J. Phys. Chem.* **1983**, *87*, 3387.
(19) Fries, P. H.; Patey, G. N. *J. Chem. Phys.* **1984**, *80*, 6253.
(20) Fries, P. H.; Jagannathan, N. R.; Herring, F. G.; Patey, G. N. *J. Chem. Phys.* **1984**, *80*, 6267.
(21) Impey, R. W.; Madden, P. A.; McDonald, I. R. *J. Phys. Chem.* **1983**, *87*, 5071-5083.
(22) Levesque, D.; Weis, J. J.; Patey, G. N. *Phys. Lett.* **1978**, *66A* (2), 115.
(23) McDonald, I. R.; Rasaiah, J. C. *Chem. Phys. Lett.* **1975**, *34* (2), 382.
(24) Patey, G. N.; Carnie, S. L. *J. Chem. Phys.* **1983**, *78* (8), 5183.
(25) Neumann, M.; Vesely, F. J; Steinhauser, O.; Schuster, P. *Mol. Phys.* **1978**, *35* (3), 841-855.
(26) Hirata, F.; Rossky, P. J.; Pettitt, B. M. *J. Chem. Phys.* **1983**, *78*, 4133.
(27) Szasz, G. I.; Heinzinger, K. *J. Chem. Phys.* **1983**, *79*, 3467 and references therein.
(28) Berkowitz, M. L.; Karim, O. A.; McCammon, J. A.; Rossky, P. J. *Chem. Phys. Lett.* **1984**, *105*, 577.
(29) Belch, A. C.; Berkowitz, M.; McCammon, J. A. *J. Am. Chem. Soc.*, preceding paper in this issue.
(30) Jorgensen, W. L. *J. Chem. Phys.* **1982**, *77*, 4156. Jorgensen, W. L.; Chandrasekhar, J.; Madura, J. D.; Impey, R. W.; Klein, M. L. *Ibid* **1983**, *79*, 926.
(31) Chandrasekhar, J.; Spellmeyer, D. C.; Jorgensen, W. L. *J. Am. Chem. Soc.* **1984**, *106*, 903. Chandrasekhar, J.; Jorgensen, W. L. *J. Chem. Phys.* **1982**, *77*, 5080.
(32) Ryckaert, J. P.; Ciccotti, G.; Berendsen, H. J. C. *J. Comput. Phys.* **1977**, *23*, 327.

0002-7863/86/1508-1762$01.50/0

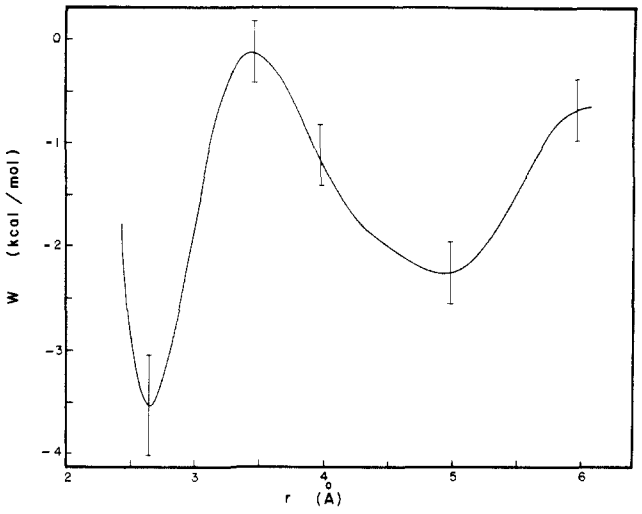

Figure 1. Potential of mean force for a sodium–chloride ion pair in water. r is the distance between ion centers.

V_{WW}^{LJ} in eq 1 is the Lennard-Jones (LJ) potential operating between the oxygen centers of the water molecules. The hydrogens are well inside the effective hard-sphere radius of the LJ potential for the oxygens. V_{WW}^{Coul} in eq 2 is the Coulomb interaction between water molecules. Here, q_i and q_j refer to the charges on different water molecules, and these charges are given in Table I. Thus, the parameters for the TIPS2 model are the A and C values for the LJ potential, the magnitude and location of the negative charge along the bisector, and the charge on the hydrogen. This model has been shown to reproduce a variety of experimental properties of water very well.[33]

The ion–ion and the ion–water interaction terms are again of the Coulomb and LJ types. The ion–water potentials are shown as follows, and the ion–ion potentials are of a similar form.

$$V_{IW}^{LJ} = \sum_{i<j} [A_S^I A_W / r_{ij}^{12} - C_S^I C_W / r_{ij}^6] \quad (3)$$

$$V_{IW}^{Coul} = \sum_{j} \sum_{\text{sites}} \frac{Q_I q_j}{r_{Ij}} \quad (4)$$

A_S^I and C_S^I in eq 3 refer to the general ion LJ parameters, and Q_I in eq 4 refers to the ionic charge. Thus Q_I refers to the sodium or the chloride ion. The values for these parameters[31] are in Table I.

Potential of Mean Force. The calculation for the solvent-averaged potential of mean force between the ions is described elsewhere,[28] and we briefly review it here for completeness. The Verlet[34] algorithm is used to simulate the molecular dynamics at 298 K. In order to generate good sampling statistics over a range of ion–ion distances, the window or umbrella sampling[35-37] technique is used. The sodium ion is assigned a very large mass and is essentially in a fixed location in the box. The chloride ion is confined to a region along and near the long axis of the box by means of a harmonic "umbrella" potential. This potential is stronger in a direction perpendicular to the ion–ion vector as compared to the direction along the vector. During the simulation, the ions therefore change their relative distance principally along the ion–ion vector. After a suitable equilibration period with the umbrella centered at some point, statistics are recorded for 10.5 ps of real time. The umbrella is then shifted, equilibration is carried out for 1.5 ps, and configurations are again recorded. The configurations are recorded every 10 steps of the simulation, or 0.015 ps apart in time. In this way,[28] the ion–ion RDF is calculated for a range of r, and the resulting potential of mean force is shown in Figure 1. The artifice of the umbrella potential has been removed analytically.

Dynamics of the Transitions. The description of the ion dynamics with special reference to solvent participation is the main content of this paper.

The ion dynamics is simulated in the following steps:

Step 1. With the setup for the equilibrium calculation described above, the ions are fixed at a distance corresponding to the top of the barrier in the potential of mean force by using a heavy sodium ion and an umbrella potential for chloride that is strong in all three dimensions. After a suitable period of equilibration, a long simulation is carried out, with periodic velocity rescaling to keep the temperature near 298 K. A molecular dynamics time step of 0.006 ps is used. Each configuration in this simulation is scrutinized and is recorded if $E_{UMB} \leq 0.5$ kJ/mol and $T = 298 \pm 10$ K, where E_{UMB} is the contribution to the total energy from the umbrella potential and T is the absolute temperature of the system. We choose these criteria in order to minimize spurious kinetic effects when the umbrella potential is removed. These recorded configurations are further scanned, and only those at least 0.3 ps apart in time are selected for use in step 2. This minimal time separation is dictated by the lifetime of the velocity autocorrelation function for water molecules. Further steps in the selection then also ensure that different types of configurations as well as different distributions of atomic momenta are sampled.

Step 2. The sodium ion is given its proper mass and all the velocities are reassigned from a Maxwellian distribution corresponding to 298 K. The simulation is run for a further 0.15 ps, any state that thereafter meets the energy and temperature criteria (as in step 1) is recorded, and the simulation is stopped. This recorded state then serves as a starting point for the generation of a trajectory in step 3.

Step 3. Each state from step 2 is taken and the umbrella potential is removed. The molecular dynamics is then run until the ion–ion radial distance corresponds to one of the minima in the potential of mean force (Figure 1). The molecular dynamics is run once more, starting from the configuration in step 2 again, this time after all the initial velocities have been reversed. This corresponds to a simulation backward in time. The simulation is again stopped when one of the minima in the potential of mean force is reached. (In some of the trajectories, the simulation is not stopped when a minimum is encountered, in order to see the subsequent behavior of the particles.) A trajectory is termed reactive or "successful" when the forward simulation and the backward simulation lead to different minima in the potential of mean force. The backward simulation is then rewritten as a "forward" simulation, for successful trajectories, and together with the original forward simulation provides a complete phase space profile of a reactive trajectory for an ion pair association/dissociation reaction. Note that no velocity (temperature) rescaling is done in steps 2 and 3. A soft energy rescaling is done in step 3 in order to correct for round-off errors. This energy scaling is really only necessary in extended runs and is rarely necessary during the simulation lifetime of an average trajectory. The energy-scaling option is used rather than temperature scaling as one would in general expect a small change in temperature as the ions move off the energy barrier between the contact and solvent-separated minima.

Preface to Analysis. To facilitate the study of solvent structure, the system is divided into seven imaginary regions.[29] These regions are determined by the ion–oxygen radial distribution functions (RDF's) around each of the ions and are shown in Figure 2. The construction is to draw hemispheres at the first and second minima of the ion–oxygen RDF's and to connect the edges using conic sections. Regions 1 and 3 are termed the "first external hydration shell" around the sodium and chloride ions, respectively. Regions 2 and 4 are the corresponding second external hydration shells. Regions 5 and 6 are between the ions, and some water molecules in these regions "hydrate" both ions simultaneously. Region 7 is the remaining part of the system, essentially bulk water. The volumes of regions 1 through 4 remain fixed, while the volumes

(33) Jorgensen, W. L. *J. Am. Chem. Soc.* **1981**, *103*, 335–340.
(34) Verlet, L. *Phys. Rev.* **1967**, *159*, 98.
(35) Pangali, C.; Rao, M.; Berne, B. J. *J. Chem. Phys.* **1979**, *71*, 2975.
(36) Northrup, S. H.; Pear, M. R.; Lee, C. Y.; McCammon, J. A.; Karplus, M. *Proc. Natl. Acad. Sci. U.S.A.* **1982**, *79*, 4035.
(37) Chandrasekhar, J.; Smith, S. F.; Jorgensen, W. L. *J. Am. Chem. Soc.* **1984**, *106*, 304.

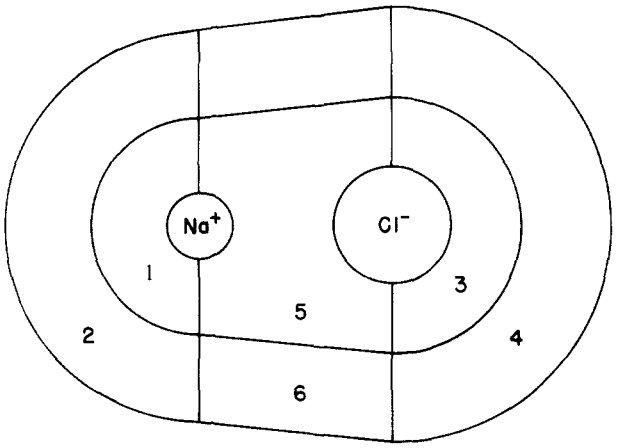

Figure 2. The imaginary regions defined around the sodium–chloride in pair.

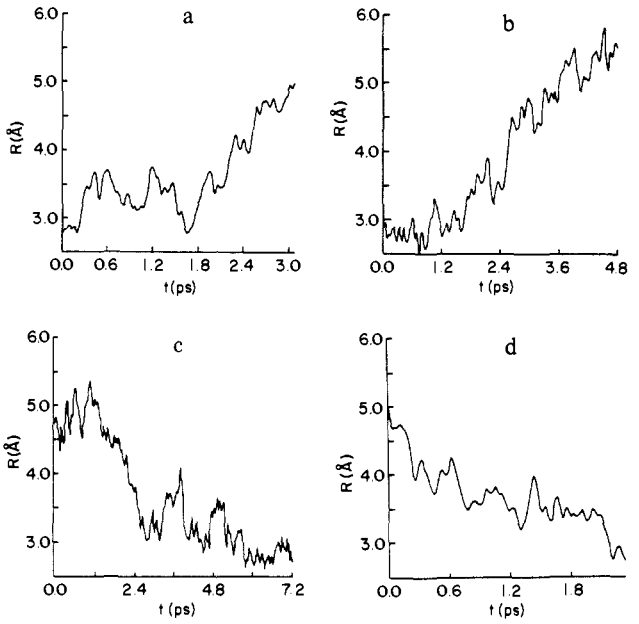

Figure 3. The interion distance as a function of time for independent trajectories: (a) trajectory A; (b) trajectory B; (c) trajectory C; (d) trajectory D.

of regions 5, 6, and 7 change with changing interion distance.

In the analysis of the dynamics, we look at several quantities in regions 1–6 as a function of time. These quantities are the number of water molecules, the number of H bonds per water molecule, and the number of ion–water "bonds" per water molecule. The hydrogen bonds as well as the ion–water bonds are determined on the basis of an energy criterion only. Two water molecules with an energy of interaction less than −2.5 kcal/mol are considered to be hydrogen bonded. If a water molecule has an interaction energy with an ion of less than −7.5 kcal/mol, the water is considered "bonded" to the ion. The criterion for ion–water bonds is empirical and satisfies the minimal requirement that ion–water bonds are confined almost entirely to the water molecules that are nearest neighbors to the ion.

Results and Analysis

Trajectories. Several independent trajectories have been generated for this process, and some of these are shown in Figure 3. The trajectories displayed in Figure 3, parts a and b will be designated "A" and "B", respectively, and discussed in detail in the subsequent sections. One can see that trajectories from one to the other minimum are of different durations, varying from 2.7 to 4.8 ps. The relative motion of the ions is diffusive in character, and in most trajectories the ions cross and recross the barrier top before eventually settling in one of the minima. This

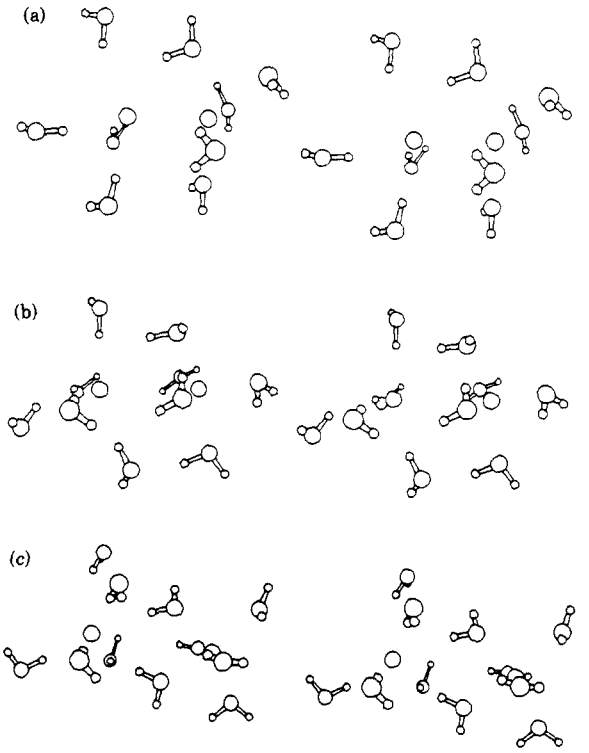

Figure 4. Instantaneous configuration of ions and surrounding water molecules for trajectory A. Only those water molecules that lie in regions 1, 3, or 5 are shown. Atom sizes are not to scale. (a) Contact geometry at 0.00 ps. (b) Transition-state geometry at 0.98 ps. (c) Solvent-separated geometry at 3.08 ps.

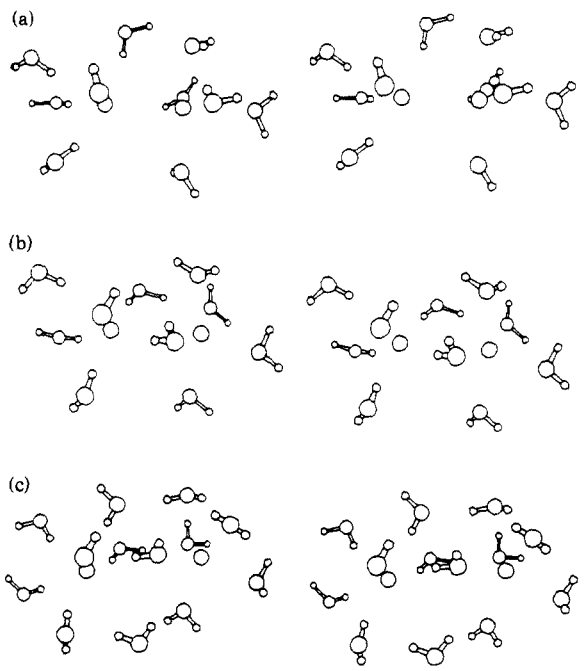

Figure 5. Instantaneous configuration of ions and surrounding water molecules for trajectory B. Only those water molecules that lie in regions 1, 3, or 5 are shown. Atom sizes are not to scale. (a) Contact geometry at 0.96 ps. (b) Transition-state geometry at 2.40 ps. (c) Solvent-separated geometry at 3.6 ps.

is roughly in accord with the estimated times for simple diffusional displacement. Taking the displacement distance, r, to be about 2 Å and the relative diffusion coefficient D to be the sum of the diffusion coefficients[38] for Na^+ and Cl^-, one has $t = r^2/6D = 2$

(38) Bockris, J. O'M.; Reddy, A. N. "Modern Electrochemistry"; Plenum Press: New York, 1970; p 296.

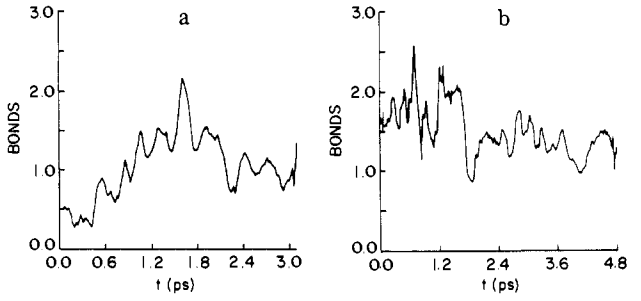

Figure 6. Number of hydrogen bonds per water molecule in region 5 as a function of time for (a) trajectory A, and (b) trajectory B.

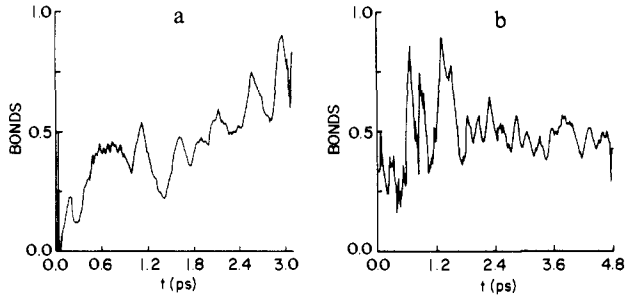

Figure 7. Number of chloride–water bonds per water molecule in region 5 as a function of time for (a) trajectory A, and (b) trajectory B.

ps. This transition then is one of diffusional crossing of a low potential barrier.

Solvent Configurations. For convenience in understanding the discussion in the following section, we first discuss the solvent configurations displayed in Figures 4 and 5. These are for two of the trajectories displayed above and serve as illustrative examples of the solvent dynamics. In both cases, the contact minimum is seen to be one in which the sodium ion is hydrated by five water molecules; together with the chloride, these waters form a strong octahedral structure around the sodium ion. In the solvent-separated state of both trajectories, at least one bridging water molecule is present in the region between the ions. These bridging water molecules have their oxygens located off the interion axis. The sodium now has its full complement of six hydrating water molecules. The transition states of the two trajectories are different, however. In the first case (Figure 4b), a water molecule belonging to the chloride first external hydration shell has entered the region between the ions. This water molecule forms a hydrogen bond with a water molecule which hydrates the sodium ion. At about the same time, another water molecule enters the first external hydration shell of chloride. In the second case, a hydrating sodium water molecule is directly influenced by the larger chloride ion and is the one that eventually enters the region between the ions to form the solvent bridge. Another water molecule enters the first external hydration shell of the sodium ion simultaneously with displacement of the bridging water.

Comparison of Trajectories. The number of hydrogen bonds per water molecule in region 5 (between the ions) is displayed as a function of time for two trajectories in Figure 6. Corresponding plots of the number of ion–water bonds per water molecule are presented in Figures 7 and 8. The value at each instant of time has been averaged over 0.132 ps to smooth these curves.

In Figure 6, hydrogen bonding for trajectory A is seen to be considerably stronger during the transition state, as compared with the contact and solvent-separated states. For this trajectory, it is also seen from Figure 7 that as the ions separate from contact to the transition state, the number of chloride–water bonds in region 5 increases. After some oscillation during the lifetime of the transition state, the chloride–water bonds finally settle to their highest value in the solvent-separated state. Correspondingly, the sodium water bonds in region 5 weaken as the transition state is achieved but thereafter show no definite behavior (Figure 8). Therefore in this trajectory ion separation from contact is assisted

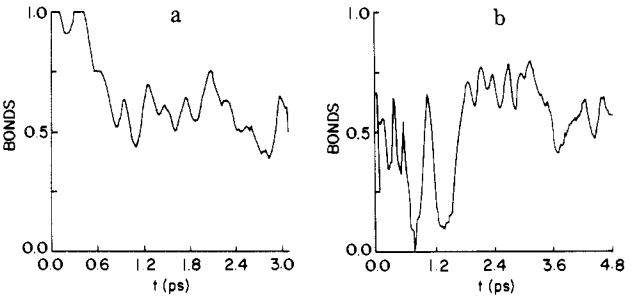

Figure 8. Number of sodium–water bonds per water molecule in region 5 as a function of time for (a) trajectory A, and (b) trajectory B.

by the entry of a chloride–hydrating water molecule into region 5. This water molecule forms new hydrogen bonds in region 5, involving the sodium-hydrating water molecules. The solvent-separated state is finally attained by the collapse of this hydrogen bonding and the entry into region 5 of the water molecule that is still bonded to the chloride ion but that also now serves as the sixth hydrating water molecule for the sodium ion.

Further examination of Figures 6–8 shows that some of the characteristics of trajectory B are quite different. First, there is no marked difference in the hydrogen bonding at the transition state as compared with the contact and solvent-separated states. Further, Figure 8 shows that for trajectory B there is an increase in the sodium–water bonds in region 5 as the ions separate from contact to the transition state; the opposite behavior is seen for trajectory A. The chloride–water bonds show little change as the ions separate from contact to the transition state in trajectory B. The subsequent behavior of the ion–water bonds is not definite as the ion separation proceeds, but the anticorrelated changes in Figures 7b and 8b suggest that the sodium-hydrating water molecules intermittently fall under the influence of the chloride ion in region 5 as the solvent-separated minimum is achieved. The fact that the hydrogen bonding in region 5 does not increase during separation from the contact to the transition state suggests that the water molecule that enters this region does so without forming any strong bonds with neighboring water molecules in this region. What does happen is that a hydrating water of the sodium ion is directly influenced by the chloride ion (rather than by another water molecule) and then plays the role of a bridging water molecule in the solvent-separated minimum. The sodium ion replaces its "lost" water molecule by another from the second hydration shell.

The mechanistic details described here are quite evident in the graphic displays of system configurations from these trajectories (Figures 4 and 5). We have discussed the two mechanisms with illustrative trajectories that are relatively simple to analyze. In general, the analysis of the trajectories is more complicated. Strong hydrogen bond fluctuations and changes in ion–water bonding in the first external hydration shells of the ions contribute to the added complexity. The dynamical role of the solvent, however, is still described by the two types of mechanism that we have discussed.

Discussion

We have analyzed in structural detail all the trajectories shown in Figure 3 and also some others not shown here. The discussion here applies to all of these trajectories. The ion dissociation process occurs through one of two mechanisms. In mechanism 1, a chloride-hydrating water forms a hydrogen bond to a water in the first shell of sodium and subsequently enters the region between the ions. In mechanism 2, a sodium-hydrating water interacts directly with the chloride and then enters the region between the ions. In each case, this leads to the formation of a solvent-separated minimum. The difference in size of the ions seems to be responsible for the obligatory hydrogen bonding step in mechanism 1.

The transition states of the two trajectories described above are relatively simple. In other cases, the hydrogen bond structure in region 5 can be somewhat more complicated, because more than

Table II. List of Trajectories[a]

label	initiation time, ps	tot lifetime, ps	TS lifetime, ps	mechanism
5001	0.000	2.4	1.2	2
1002	0.924	3.1	1.56	1
9002	5.71	1.7	0.12	2
2003	6.95	4.8	3.6	1
1004	7.99	2.7	0.6	2
1005	11.88	2.4	0.0	2

[a] Time step of dynamics = 0.006 ps. The trajectories labeled 1002, 1004, 2003, and 5001 are displayed in Figure 3 parts a–d, respectively.

one hydrogen bond connecting the sodium and chloride hydration shells can exist in region 5 at any given time. As long as strong hydrogen bonds of this kind exist, the transition state continues. The breaking of the transition-state hydrogen bonds occurs through the interference of the second-shell water molecules, which are relatively mobile and can act to break existing bonds while not being themselves involved directly in the structural changes. In mechanism 2, the second hydration shell also plays a role in supplying a replacement water molecule for the sodium ion first hydration shell when the transition state decays to the solvent-separated state. The strong tendency of the sodium ion to maintain octahedral coordination is evident here and in other detailed aspects of the transitions. The chloride first hydration shell is relatively less stable and well-defined and does not play as critical a role in the dynamics, except as a source of bridging water in mechanisms of type 1.

Listed in Table II are some relevant numbers of the other trajectories we have studied. This preliminary study shows that the conditions that determine the type of mechanism do not appear to persist for times greater than 1 ps and suggests that mechanism 2 dominates the reaction path.

One might imagine that polarization fluctuation[39-42] in the solvent could influence the dynamics here, as for example in chemical reactions involving reactant charge redistribution. However, bulk-solvent polarization has strong competition here from steric and hydrogen bonding interactions. Examination of solvent polarization fluctuations (not shown) indicates that these do not determine the ion displacements.

Having studied the solvent–ion dynamics, it is instructive to make a comparison with the equilibrium solvation structure. In that work,[29] the solvent structure as the ions separate is described as a tilting of the octahedron around the sodium ion. This tilting apparently allows a sodium-hydrating water molecule at the transition state to attempt to penetrate between the sodium ion and the chloride ion as a possible step toward achieving a solvent-separated minimum. This interpretation of the equilibrium solvation structure seems accurate when applied to the actual dynamics of the reaction. In the dominant reaction mechanism discussed in the present work, labeled mechanism 2, the solvent bridge in the separated minimum indeed involves one of the water molecules which also hydrates the sodium ion in the contact minimum. A solvent depletion in region 1 is also observed in dynamical trajectories, as the ions move from contact to the transition state. It can be seen from the dynamical plots of solvent numbers (not shown here) that the water molecules that are "lost" from region 1 enter region 5 as the transition state is achieved. The hydrogen bond structure around the ions is not always similar in the equilibrium and the dynamical cases. In most of the trajectories listed in Table II, the dynamical hydrogen bond graphs (not shown here) show a relatively larger hydrogen bonding in region 1 at the transition state as compared with the contact and the separated states. The opposite is seen in the equilibrium study. It should be remarked at this point that the dynamical solvent structures we have discussed correspond to those special cases where the achievement of the transition state leads to an eventual passage to the other minimum. In the equilibrium calculations, all the solvent structures are averaged, including the ones corresponding to unsuccessful trajectories. The equilibrium results therefore need not correspond exactly to the dynamical ones.

Concluding Remarks

We have studied in detail the ion association/dissociation reaction for a sodium chloride ion pair in water. Using several independent trajectories, we have described the role of the solvent in the dynamics of these transitions and have proposed two main structural mechanisms for the solvent participation in the dynamics.

Electronic polarizability is not included in the TIPS2 model explicitly. This can be expected to influence the results to some extent; it is likely that the structural dynamics will not be significantly affected, although the average solvent-separated structure may be slightly different in terms of the detailed arrangement of the water molecules. One possible change would be in the relative position of the separating water molecules, which will however still belong to the octahedral first hydration shell of the sodium ion.

In terms of potential energy surfaces, there will be many possible distinct transition states, although most of these will likely fall into the two general classes identified here. A more quantitative/statistical analysis of the transition states could be performed,[43-47] where multiple transition states are studied in terms of the local potential minima available to the system and the low-energy pathways that connect these minima.

Rate constants for the forward and reverse processes can also be determined. Generation of necessary trajectories for this determination is computationally demanding, and work is in progress along these lines.

Acknowledgment. We thank Professors Max Berkowitz, Bill Jorgensen, and Peter Rossky for stimulating discussions. This work has been supported in part by grants from the Robert A. Welch Foundation and NSF. J.A.M. is a Camille and Henry Dreyfus Teacher–Scholar.

Registry No. NaCl, 7647-14-5.

(39) van der Zwan, G.; Hynes, J. T. *J. Chem. Phys.* **1982**, *76*, 2993.
(40) Calef, D. F.; Wolynes, P. G. *J. Chem. Phys.* **1983**, *78*, 470.
(41) van der Zwan, G.; Hynes, J. T. *Chem. Phys. Lett.* **1983**, *101*, 367.
(42) van der Zwan, G.; Hynes, J. T. *Physica A: (Amsterdam)* **1983**, *121A*, 227.
(43) Stillinger, F. H.; Weber, T. A. *Phys. Rev. A* **1982**, *25* (2), 978.
(44) Stillinger, F. H.; Weber, T. A. *Phys. Rev. A* **1983**, *28* (4), 2408.
(45) Weber, T. A.; Stillinger, F. H. *J. Chem. Phys.* **1984**, *80* (6), 2742.
(46) Stillinger, F. H.; Weber, T. A. *J. Chem. Phys.* **1984**, *80* (9), 4434.
(47) Stillinger, F. H. *J. Phys. Chem.* **1984**, *88*, 6494.